ISSN 0006-2979, Biochemistry (Moscow), 2009, Vol. 74, No. 8, pp. 910-916. © Pleiades Publishing, Ltd., 2009.
Published in Russian in Biokhimiya, 2009, Vol. 74, No. 8, pp. 1117-1125.

Binding of ATP and Its Derivatives to Selenophosphate Synthetase from *Escherichia coli*

Y. V. Preabrazhenskaya[1,2]*, I. Y. Kim[1], and T. C. Stadtman[1]

[1]*Laboratory of Biochemistry, National Heart, Lung and Blood Institute, National Institutes of Health, 9000 Rockville Pike, Bethesda, MD 20892, USA*
[2]*Department of Biology and Ecology, Grodno State University, 3/1 Dovatora, Grodno 230015, Belarus; E-mail: yuliya.preabrazh@gmail.com*

Received March 21, 2008
Revision received March 3, 2009

Abstract—Mechanistically similar selenophosphate synthetases (SPS) have been isolated from different organisms. SPS from *Escherichia coli* is an ATP-dependent enzyme with a C-terminal glycine-rich Walker sequence that has been assumed to take part in the first step of ATP binding. Three C-terminally truncated mutants of SPS, containing the N-terminal 238 (SPS_{238}), 262 (SPS_{262}), and 332 (SPS_{332}) amino acids of the 348-amino-acid protein, have been extracted from cell pellets, and two of these (SPS_{262} and SPS_{332}) have been purified to homogeneity. SPS_{238} has been obtained in a highly purified form. Binding of the fluorescent ATP-derivative TNP-ATP and Mn-ATP to the proteins was examined for all truncated mutants of SPS and a catalytically inactive C17S mutant. It has been shown that TNP-ATP can be used as a structural probe for ATP-binding sites of SPS. We observed two TNP-ATP binding sites per molecule of enzyme for wild-type SPS and SPS_{332} mutant and one TNP-ATP binding site for SPS_{238} mutant. The stoichiometry of Mn-ATP-binding was 2 mol of ATP per mol of protein determined with [^{14}C]ATP by HPLC gel-filtration column chromatography under saturating conditions. The binding stoichiometries for SPS_{332}, SPS_{262}, and SPS_{238} were 2, 1.6, and 1, respectively. The C17S mutant exhibits about one third of wild type SPS TNP-ATP-binding ability and converts 12% of ATP in the ATPase reaction to ADP in the absence of selenide. The C-terminus contributes two thirds to the TNP-ATP binding; SPS_{238} likely has one ATP-binding site removed by truncation.

DOI: 10.1134/S0006297909080136

Key words: selenophosphate synthetase, truncated mutants, ATP-binding, fluorescence enhancement

Selenophosphate synthetase (SPS) (EC 2.7.9.3) is a key enzyme of the selenium pathway in the cell. It is an ATP-dependent enzyme that forms selenophosphate, AMP, and orthophosphate in 1 : 1 : 1 ratio stoichiometrically from ATP and selenide [1, 2]:

$$ATP + HSe^- + H_2O \rightarrow H_2SePO_3^- + AMP + P_i.$$

The selenophosphate is derived from the γ-phosphoryl group of ATP, and the β-phosphoryl group is converted to orthophosphate [1, 3]. In the absence of selenide, SPS quantitatively converts ATP to AMP and two orthophosphates [1]. The first step in this multi-step reaction has been postulated as production of a pyrophosphoryl–enzyme intermediate with cleavage of ATP to γP_i and AMP. However, positional isotope exchange experiments (PIX) did not confirm this suggestion but showed formation of an enzyme–phosphoryl intermediate in the first step as a result of a nucleophilic attack by the enzyme on the γ-phosphoryl group of ATP [4]. Direct evidence of the existence of a covalent enzyme intermediate in PIX was observed in the absence of selenide. Therefore, in this study we investigate the first step of the SPS catalytic mechanism paying particular attention to ATP-binding in the absence of selenide.

Abbreviations: CHAPSO, 3-[(3-cholamidopropyl)dimethylammonio]-1-propanesulfonate oxide; Gu-HCl, guanidine hydrochloride; PIX, positional isotope exchange; SPS, selenophosphate synthetase; TNP-ATP, 2′(3′)-O-(2,4,6-trinitrophenyl)adenosine 5′-triphosphate.

* To whom correspondence should be addressed.

MATERIALS AND METHODS

Materials. Taq DNA polymerase from Gibco-BRL (USA), restriction enzymes from New England Biolabs

(USA), modified T_7 DNA polymerase (Sequenase) from United States Biochemical (USA), [γ-^{33}P]ATP (3000 Ci/mmol) from Perkin Elmer (USA), [8-^{14}C]ATP from ICN (USA), a fluorescent derivative of ATP, TNP-ATP (2′(3′)-O-(2,4,6-trinitrophenyl)adenosine 5′-triphosphate), from Molecular Probes (USA), SeeBlue Pre-Stained Protein Standard from Invitrogen (USA), and the detergent 3-[(3-cholamidopropyl)dimethylammonio]-1-propanesulfonate oxide (CHAPSO) from Sigma (USA) were used in this study. All the other chemicals were of the highest grade available.

Strain and plasmids. SPS, the product of the *selD* gene, and the C17S protein, the product of a *selD* mutant gene, were produced in *Escherichia coli* strain MB08 transformed with corresponding plasmids as reported previously [5, 6]. Truncation of the *E. coli selD* gene from the C-terminus using the polymerase chain reaction (PCR) technique was performed as follows. We constructed three differently sized *selD* genes: 724, 799, and 993 bp, encoding for SPS_{238}, SPS_{262}, and SPS_{332}, respectively (Scheme).

The DNA sequence of forward oligonucleotide primer used in common for the three mutants was 5′-ATGAGCGAGAACTCGATTCGT-3′. The sequences of backward oligonucleotide primer containing stop codon, TAA, were: for SPS_{238}, 5′-TGACACATTTAGCTCAAGTGG-3′; for SPS_{262}, 5′-ACTTAATGTACTCTTAAACAC-3′, and for SPS_{332}, 5′-CAATTGCCGTCAGTTAAATGC-3′.

The PCR reactions were performed in a Perkin Elmer thermal cycler. The reactions for amplification of truncated DNAs were performed as follows: denaturation at 94°C for 1 min, hybridization at 55°C for 1 min, and chain polymerization at 72°C for 2 min. The reactions were allowed to proceed for 35 cycles. The plasmid pMN340 was used as the template DNA [7]. The PCR products were analyzed on a 1% agarose gel. Plasmid pMN340 carrying the ampicillin-resistant gene and *selD* gene behind the T_7 promoter [3], which was used as a *selD* gene source, was a gift from A. Bock (University of Munich, Germany).

Each PCR product was ligated into pCR2.1 vector (Invitrogen, USA). The recombinant pCR2.1 plasmids were amplified, purified, and then digested with *EcoR*I. The *EcoR*I DNA fragments containing the truncated *selD* genes were subcloned into plasmid pKK233.2 (Pharmacia, Sweden). The resulting plasmids containing each truncated *selD* gene were named pKK-SPS_{238}, pKK-SPS_{262}, and pKK-SPS_{332}, respectively. The recombinant plasmids were then transformed into *E. coli* MB08 [5] to analyze their biological activities.

Overexpression and purification of WT SPS and the truncated mutants. MB08 cells transformed with corresponding plasmids were grown aerobically in 1-liter flasks with vigorous stirring in Luria–Bertani + ampicillin medium until A_{600} reached 0.6. At that time, IPTG (isopropyl β-D-thiogalactoside) was added to a final concentration of 1% to induce overexpression of the SPS SelD truncated mutants. The product of the *selD* gene, WT SPS, was purified as described [8] with some modifications. DEAE-Sepharose chromatography was used after an ammonium sulfate fractionation step followed by phenyl-Sepharose and butyl-Sepharose chromatography. The SPS SelD truncated mutants were extracted from the pellets and purified similarly to WT SPS with one exception, that the ammonium sulfate fractionation step after dissolving of SPS_{238} with 5 M guanidine hydrochloride (Gu-HCl) was not applied. The isolated proteins were monitored for purity by electrophoresis in SDS-polyacrylamide gels.

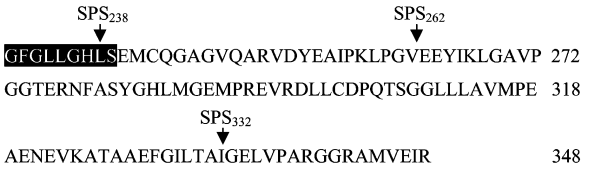

Primary structure of the C-termini of the SPS truncations. Locations of the truncation for the C-termini of SPS_{238}, SPS_{262}, and SPS_{332} are indicated with black arrows. The proposed ATP-binding region is shown with a black background

TNP-ATP binding to WT and mutant SPS. The recombinant wild-type *selD* gene product in *E. coli* and the mutants were tested for structural integrity with a fluorescent analog of ATP, TNP-ATP. The fluorescence enhancement of TNP-ATP upon binding to the protein was measured in 25 mM Tris-HCl, 100 mM NaCl, 30 mM KCl, 10 mM $MgCl_2$, pH 7.0, using a PTI fluorimeter. The excitation wavelength was 408 nm, and emission spectra were scanned from 500 to 600 nm. The amount of fluorescence enhancement was determined by subtracting the fluorescence of free dye (TNP-ATPf) from the fluorescence of the sample containing protein. For protein-free samples, the fluorescence intensity equates with the concentration of the ligand. For protein-containing samples at concentrations of the protein much higher than K_d, fluorescence is given by the concentration of the ligand multiplied by the fluorescence intensity enhancement factor, γ [9]. Thus, the value of the fluorescence intensity enhancement factor γ was defined as a ratio of the slopes in plots of fluorescence intensity versus TNP-ATP concentration in samples containing the concentrated solution of protein (124 μM) and in protein-free samples. At such high protein concentrations, essentially all the fluorophore is bound. The binding stoichiometries (n) were estimated from the calculated X-axis intercepts of the Scatchard plots, and equilibrium binding constants (K_d) were estimated from the slopes [10]. Data of fluorescence titration were presented graphically and analyzed using the GraphPad Prism 4.00 program (GraphPad Software, USA).

Mn-ATP binding to the proteins. Reaction mixtures (100 µl) containing 100 mM Tricine-KOH, pH 8.0, 30 mM KCl, 0.5 mM dithiothreitol (DTT), 4 mM $MnCl_2$, 0.5 mM [^{14}C]ATP (1 µCi), 4.5 mM ATP, and 57 µM protein were incubated at 23°C for 10 min. The whole reaction mixture was then applied to a TSK-gel HPLC column S2000 SW pre-equilibrated with 100 mM Tricine-KOH (pH 8.0) buffer containing 0.5 mM DTT and 4 mM $MnCl_2$. The same buffer was used for the elution. The flow rate was 1 ml/min, and 1-ml fractions were collected. The radioactivity of a 100-µl aliquot of each fraction was measured by liquid scintillation spectroscopy. Protein concentration was monitored by absorption measurements at 280 nm and calculated using ε_{280} = 16,100 $M^{-1}\cdot cm^{-1}$ [11]. The amount of radioactive ATP in the protein peak fractions is termed "Mn-ATP bound".

ATPase activity of SPS. The rate of AMP or ADP production in the absence of selenide was assayed as described [4] with some modifications. Typically, 0.1 M Tricine-KOH (pH 8.0) and 2 mM $MnCl_2$ were used. After stopping the reaction by heating to 95°C and separating the protein by centrifugation through 0.45 µm Amicon (USA) centrifugal filter units, 50 µl aliquots were injected onto an Apex C_{18} (5 µm) column to separate nucleotides by ion-pair HPLC chromatography in 0.1 M TEA (triethylamine bicarbonate) buffer, pH 5.7.

To measure time-course of Mn-ATPase activity, a reaction mixture sample (500 µl) containing 37 µM of WT SPS or C17S mutant, 3.3 mM [γ-^{33}P]ATP (20 µCi), and the components described above for Mn-ATPase activity was incubated at 37°C. Aliquots of 100 µl were taken each 20 min, heated to 95°C, filtered, and loaded onto a reverse-phase HPLC column to separate AMP, ADP, and ATP [4]. The radioactivity in nucleotide fractions was determined by liquid scintillation. The amount of ^{33}P eluted with the ATP peak corresponded to ATP recovered.

RESULTS

Overexpression and purification of SPS truncated mutants. IPTG was added to induce expression of the 25-kDa SPS_{238}, 29-kDa SPS_{262}, and 34-kDa SPS_{332}. The expression of all three proteins in *E. coli* has shown that they are located in the insoluble part of the extract when grown at 37°C for 10 h. SPS_{332} becomes soluble if the bacteria are grown at 28°C for 2 h following the IPTG addition (Fig. 1; see color insert). SPS_{262} is soluble when the bacteria are grown at higher pH 7.8 (the protein has higher p*I* = 5.78 instead of 5.20 for WT).

WT, SPS_{262}, and SPS_{332} were purified to homogeneity by a four-step purification procedure as judged by SDS-PAGE (not shown). The pellet containing SPS_{238} was solubilized by addition of 5 M Gu-HCl. It has been found recently that under increasing concentrations of Gu-HCl solution (0-6 M) a Se-binding protein from *Methanococcus vanelii* with structure similar to SPS can be partially unfolded and then restored by overnight dialysis [12]. However, although upon unfolding of WT SPS in 6 M guanidine the spectrum of the chromophore was retained [12], no divalent cation-dependent shift was observed in the presence of 6 M guanidine, and removal by dialysis failed to restore the activity of the enzyme [11]. In our experiments, after dissolving SPS_{238} with 5 M guanidine and dialysis, the enzyme was kept in solution by addition of CHAPSO detergent to the buffer that facilitates correct refolding [13]. The detergent was then removed by repeated washing on an Amicon Centriprep centrifugal filter device (YM-10 membrane, 10,000 MWCO), and SPS_{238} was recovered by immunoaffinity chromatography on a BrCN-Sepharose matrix. The bound antibodies were produced in sheep against WT SPS. About 1.5 mg of highly purified SPS_{238} per liter of culture was recovered.

TNP-ATP binding to SPS and mutant proteins. To determine the number of ATP-binding sites, we used a fluorescent derivative of ATP, TNP-ATP, that binds to hydrophobic ATP-binding sites of kinases and some phosphatases [14]. Its absorption spectrum reveals a large absorption peak at 408 nm. Using an excitation wavelength of 408 nm, we observed fluorescence enhancement and a spectral shift to the red upon addition of SPS (Fig. 2).

To measure TNP-ATP binding quantitatively, we determined that the calibration curve for the free TNP-ATP is linear. To estimate the affinity of SPS to TNP-ATP, we obtained titration curves of the ligand and the

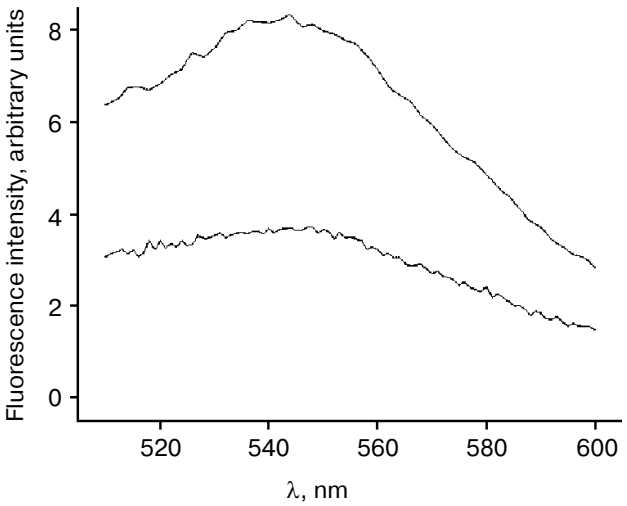

Fig. 2. Fluorescence enhancement of TNP-ATP upon binding to SPS (WT). The upper spectrum represents the fluorescence emission (λ_{max} ~ 540 nm) of a sample containing 4 µM TNP-ATP and 2 µM wild-type SPS in 25 mM Tris-HCl, 100 mM NaCl, 30 mM KCl, 10 mM $MgCl_2$, pH 7.0. The lower spectrum is for 4 µM TNP-ATP in the absence of SPS.

complex (Fig. 3). If one compares the data for titration of free dye (TNP-ATPf) and the dye–enzyme complex, the fluorescent enhancement gives the amount of TNP-ATP bound (TNP-ATPb). Typically used to determine dissociation constant (K_d) and the number of binding sites (n), the Scatchard plot for WT SPS is shown in Fig. 4. As seen from Table 1, the number of binding sites does not decrease for the mutant SPS_{332} in comparison to WT although the K_d value for TNP-ATP is 4 times higher. Such a significant increase in K_d could indicate that a significant conformational change occurs due to truncation leading to the insolubility of the protein. However, identical TNP-ATP binding properties and identical fluorescence yields were observed for WT SPS not-treated with Gu-HCl and for WT SPS unfolded with 5 M Gu-HCl and then refolded as described in "Materials and Methods". This is evidence that after solubilization by 5 M Gu-HCl the purified WT SPS does correctly refold upon dialysis in the presence of CHAPSO. Binding stoichiometries measured for two longer truncated mutants, SPS_{332} and SPS_{262}, are within 30% of the value documented for wild-type SPS, indicating that these mutants retain substantial structural integrity in contrast to SPS_{238} and C17S mutants. The latter appear to have about one binding site for TNP-ATP. Moreover, the dissociation constants (to Mg-ATP) for SPS_{238} and C17S are higher than these for SPS_{332} and SPS_{262} (Table 1). Thus, the shorter truncated mutant (SPS_{238}) and C17S demonstrate lower affinity to ATP. SPS_{238} probably has one ATP-binding site removed by truncation.

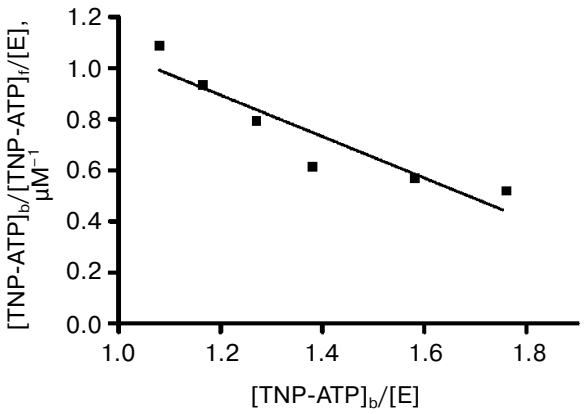

Fig. 4. Scatchard plot for TNP-ATP binding to WT SPS. $[TNP\text{-}ATP]_b$ and $[TNP\text{-}ATP]_f$ represent the concentration of enzyme-bound (E) and free TNP-ATP, respectively.

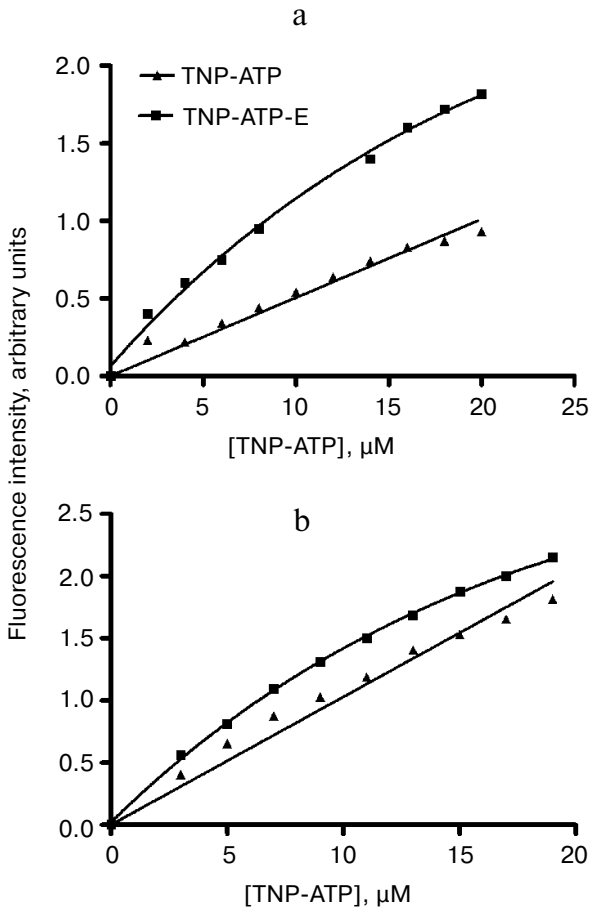

Fig. 3. Fluorescence titration of SPS_{332} with TNP-ATP. TNP-ATP binding to SPS_{332} (2 μM) was performed in (a) K^+ medium containing 100 mM Tricine-KOH, 30 mM KCl, and 10 mM $MgCl_2$, pH 7.0, and (b) Na^+ medium containing 30 mM NaCl instead of KCl. Fluorescence responses were determined for the protein-free sample (TNP-ATP) and enzyme-containing sample (TNP-ATP-E) after each sequential addition of TNP-ATP. Fluorescence was measured at 540 nm.

During the detection of conformational changes upon addition of metal ions we found that TNP-ATP exhibited two times higher affinity to WT SPS in potassium-containing medium (Fig. 3a) than in sodium-containing medium (Fig. 3b). The data correlate with those obtained earlier on the SPS activity that is also twice as high when K^+ is present in the reaction mixture instead of Na^+ [1, 15].

Most interestingly, the addition of Mg-ATP in the medium induced a decrease in the TNP-ATP fluorescence, which indicated a displacement of bound TNP-ATP by ATP. The K_d (for Mg-ATP) was calculated from this competition for all the proteins (Table 1). The competitive displacement of TNP-ATP with the main substrate for SPS, Mg-ATP, could also be followed by increase in ATPase activity. Figure 5 shows the effect of Mg-ATP in the preincubation solution on inhibition of the activity of the enzyme preincubated with TNP-ATP. ATP displaces TNP-ATP in the active site at high concentrations. EC_{50} determined from the plot is close to the K_m for Mg-ATP [16]. This might mean that there is a competition between the substrate and the inhibitor in the active site.

Mn-ATPase activity. A detailed analysis of Mn-ATPase activity has been carried out in order to deter-

Table 1. Summary of equilibrium binding parameters and some kinetic constants for wild-type and truncated SelD mutants to substrate analog TNP-ATP and to ATP

Enzyme	K_d (TNP-ATP), μM	*n**	K_d (Mg-ATP), μM**	K_m (Mn-ATP), mM***	V_{max}***, nmol/min
WT	1.22 ± 0.15	2.28 ± 0.12	239 ± 3	1.6 ± 0.05	3.63 ± 0.17
SPS_{332}	5.24 ± 0.02	2.1 ± 0.07	430 ± 30	5.2 ± 0.07	3.32 ± 0.10
SPS_{262}	10.1 ± 0.05	1.85 ± 0.15	430 ± 30	7.7 ± 0.04	2.17 ± 0.09
SPS_{238}	23.2 ± 0.8	1.15 ± 0.11	550 ± 50	10.3 ± 0.1	0.12 ± 0.01
C17S	2.85 ± 0.16	1.56 ± 0.11	1050 ± 70	n.d.	n.d.

Note: n.d., not determined.

* *n* is binding stoichiometry for TNP-ATP binding calculated from X-axes intersection points of the Scatchard plots.

** K_d (Mg-ATP) was calculated in competitive displacement experiments by titration of TNP-ATP–enzyme complex with Mg-ATP.

*** Enzyme concentration was 37 μM.

mine kinetic parameters for the reaction and saturating conditions for Mn-ATP-binding. The calibration curve for AMP determination by HPLC was linear over a 20-fold concentration range, and nanomolar amounts of product could be detected (not shown). This is in accordance to the linear dependence of AMP formation obtained earlier under similar conditions, but for Mg-ATPase activity [17]. Therefore, AMP production can be used for the HPLC activity assay method presented. Kinetic constants, K_m (Mn-ATP) and V_{max}, are shown in Table 1. For WT SPS we obtained K_m for Mn-ATP about two times higher (1.6 mM) than for Mg-ATP (0.9 mM). The rate of the reaction under these conditions (pH 8, 37°C) appears to be the same as during Mg-ATP hydrolysis performed in the presence of selenide but at room temperature.

To obtain a time course for the reaction of Mn-ATP hydrolysis, we determined the amount of γ-^{33}P recovered in [γ-^{33}P]ATP fraction during hydrolysis as a function of the reaction time (Table 2). The formation of products from the SPS reaction was monitored by using a reverse-phase HPLC column as in the ATPase assay described under "Materials and Methods". The peak of radioactive [γ-^{33}P]ATP that remained non-hydrolyzed superimposed the peak of total ATP obtained after separating ATP, ADP, and AMP (not shown). As can be seen from Table 2, Mn-ATP hydrolysis is practically complete after 1 h of reaction at 37°C (only 4% of the radioactive ATP was not used). Interesting data were obtained for the hydrolysis of Mn-ATP by C17S mutant – after 1 h about 12% of the free [γ-^{33}P]ATP was not recovered due to its possible hydrolysis (Table 2). The absorbance profile at 260 nm after C_{18} column chromatography revealed a detectable peak of ADP and near absence of AMP peak (data not shown). A slow catalytic exchange between ADP present in the reaction mixture after hydrolysis by C17S and ATP can be assumed. The results are similar to those obtained for WT SPS carrying out the catalytic exchange between [^{14}C]ADP and ATP [4]. Thus, ADP may be an intermediate in the SPS reaction; C17S mutant does not possess the selenophosphate-making activity [6] but can hydrolyze ATP to ADP.

Table 2. Hydrolysis of [γ-^{33}P]ATP by SPS in the absence of selenide*

Time, min	C17S	WT
	ATP hydrolyzed, cpm (% conversion)**	ATP recovered, cpm (%)
20	236 400 (3.2)	174 000 (20.6)
40	286 800 (5.9)	67 600 (10.6)
60	398 200 (12.3)	23 960 (4.4)

* The data are given after correction for the blank that does not contain protein.

** ATP hydrolyzed was determined as the difference between ATP loaded onto the column and ATP recovered.

Mn-ATP-binding. Figure 6 reveals Mn-ATP binding to the WT SPS enzyme as ^{14}C-containing fractions elute from the gel-filtration column together with the protein peak containing bound Mn-ATP (peak *1*). The molar ratio ATP/enzyme quantified from this radioactive assay gives the amount of 13.8 nmol ATP per 7.0 nmol enzyme, which is equivalent to about 2 molecules of Mn-ATP bound to 1 molecule of the WT SPS. In profiles similar to that shown in Fig. 6, the data of Mn-ATP binding to all the mutants were obtained. They are summarized in Table 3 and typically agree with the data obtained using the fluorescent derivative TNP-ATP (Table 1).

DISCUSSION

Based on earlier information about the properties of selenophosphate synthetases (SPS) from different sources, at least one Walker motif (a conserved glycine-rich ATP-binding sequence) is located in the C-terminal region of all SPS [18]. We created truncated C-terminal regions of mutant ATP-binding sites of SPS to determine if the Walker sequence was required for Mn-ATPase activity. It has been shown for *E. coli* SPS that Cys17 located in the glycine-rich sequence of the N-terminal region of the protein (-Gly-Ala-Gly-Cys[17]-Gly-Cys-Lys-Ile-) is essential for SPS activity [6]. Accordingly, the Cys17 mutant does not catalyze biosynthesis of selenophosphate; however, the mutant still exhibits 1/3 ATPase activity of WT SPS. In addition, ADP is formed preferentially instead of AMP. The catalytic mechanism of SPS derived from PIX supports the idea of residual ADP in the active site following cleavage of ATP [4, 19]. Therefore, it is likely that the Cys17 mutant still catalyzes the first step of the aforementioned reaction.

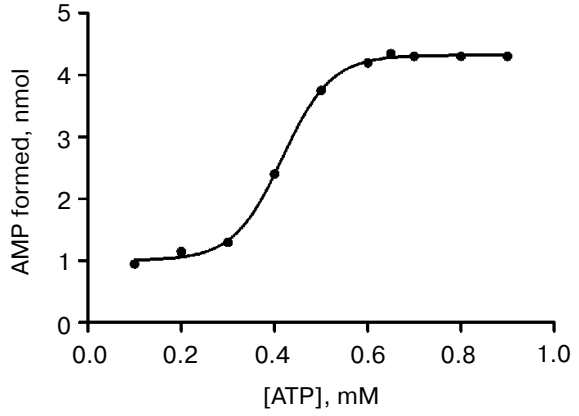

Fig. 5. Competitive displacement of TNP-ATP with Mg-ATP. ATP protects against TNP-ATP inhibition of ATPase activity of SPS_{332}. SPS_{332} (3.14 μM) was suspended in 25 mM Tris-HCl, 30 mM KCl, 100 mM NaCl, pH 8.0, and 10 μM TNP-ATP. The suspensions were incubated in the presence of varied concentrations of Mg-ATP at 37°C and placed on ice. Then ATPase activity was determined as described under "Materials and Methods".

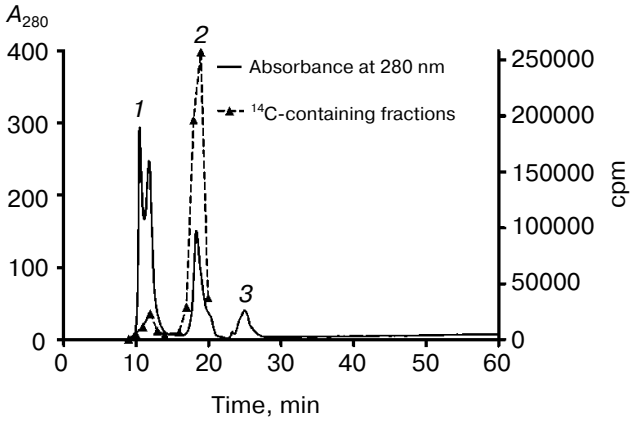

Fig. 6. Mn-ATP binding to WT SPS (gel-filtration chromatography on HPLC S2000 SW column). The peaks eluted are interpreted as follows: *1*) protein peak; *2*) ATP peak; *3*) DTT.

Table 3. Mn-ATP/enzyme binding ratio and fluorescence enhancement factor upon binding of TNP-ATP to the enzymes

Enzyme	Mn-ATP bound, nmol/nmol enzyme	Factor γ*
WT	1.97	16.2
SPS_{332}	1.79	12.3
SPS_{262}	1.6	11.1
SPS_{238}	1.07	9.97
C17S	1.36	4.58

* Factor γ is defined as a ratio of respective fluorescence responses for bound and free TNP-ATP and is obtained as the ratio of initial slopes in fluorescence versus [TNP-ATP] plots for a sample containing concentrated protein and no protein, respectively [9].

The TNP-ATP-binding ability of the C17S mutant in the absence of selenide is 1/3 that of WT under the same reaction conditions. However, the results of 8-azido-ATP-binding to the WT SPS and its mutants obtained previously [20] showed very low ATP derivative binding to C17S, C19S, and C17,19S mutants although Mn-[^{14}C]ATP binding to C17S mutant was almost unchanged in comparison to WT. Apparently, the mutations in position 20, K20R and K20Q, significantly decreased Mn-ATP binding in that study.

The recent sequence alignment of N-terminal region of SPS containing glycine-rich sequence identified longer conserved regions [21] than had been reported previously [18]. The highly conserved region starting from Gly16 in α-helix or loop conformation ending with Ser22 for at least four bacterial SPS is very similar to ATP-binding sites of different ATPases.

It is much more likely that SPS has at least two sites catalyzing ATP hydrolysis. The results with the fluorescent derivative of ATP, TNP-ATP, are confirmatory. First, we obtained three times lower fluorescence enhancement for the C17S mutant. Second, the data from Scatchard plot obtained for WT and SPS_{332} truncated mutant indicated two TNP-ATP-binding sites. ATP protects against TNP-ATP inhibition with half-maximal protection at 0.47 mM. This does not agree with the data obtained for the protein with one ATP-binding site [22] when TNP-ATP affinity is usually higher. However, there

is evidence of competitive displacement of TNP-ATP by ATP due to similar affinity for ATPase containing two nucleotide binding sites [23].

The dissociation constant for TNP-ATP to SPS_{262} is five times higher than that of WT. This is possibly due to truncation of a rather large part of the protein molecule. Increasing of dissociation constant could be evidence of structural change leading to inclusion body formation. Thus, SPS_{238} mutant has K_d to TNP-ATP of 20 μM in comparison with 1 μM for WT and can be obtained in the soluble part of the extract after dissolving the inclusion bodies with 5 M Gu-HCl.

There is also data indicating that binding to ATP-agarose determined for the WT SPS and mutant C17S is unimpaired with the mutation [6]. Soti et al. [24] obtained very similar data on the heat shock protein Hsp90 binding to ATP-Sepharose, indicating Hsp90 has two ATP-binding sites with different affinities. Therefore, they can only be distinguished with TNP-ATP as far as TNP-ATP accesses the C-terminal cryptic site without the need for an occupied N-terminal site [24].

The most essential part for ATPase activity seems to be present in the shortest truncated mutant, SPS_{238}. The number of TNP-ATP binding sites is reduced to one. These data were also confirmed with quantitative radioactive assay where the ratio of ATP bound per molecule of protein decreases from two for WT and SPS_{332} mutant to one for SPS_{238} mutant.

The results of truncation of SPS from C-terminus have shown the C-terminus contributes to the ATP-binding by SPS. The SPS_{238} mutant is unlikely to contain both ATP-binding sites; possibly one is eliminated by truncation.

REFERENCES

1. Veres, Z., Kim, I. Y., Scholz, T. D., and Stadtman, T. C. (1994) *J. Biol. Chem.*, **269**, 10597-10603.
2. Lacourciere, G. M., Mihara, H., Kurihara, T., Esaki, N., and Stadtman, T. C. (2000) *J. Biol. Chem.*, **275**, 23769-23773.
3. Ehrenreich, A., Forschhammer, K., Tormay, P., Veprek, B., and Boeck, A. (1992) *Eur. J. Biochem.*, **206**, 767-773.
4. Walker, H., Ferretti, J. A., and Stadtman, T. C. (1998) *Proc. Natl. Acad. Sci. USA*, **95**, 2180-2185.
5. Leinfelder, W., Forschhammer, K., Zinoni, F., Sawers, G., Mandrant-Berthelott, M.-A., and Boeck, A. (1988) *J. Bacteriol.*, **170**, 540-546.
6. Kim, I., Veres, Z., and Stadtman, T. C. (1992) *J. Biol. Chem.*, **267**, 19650-19654.
7. Leinfelder, W., Forschhammer, K., Veprek, B., Zehelein, E., and Boeck, A. (1990) *Proc. Natl. Acad. Sci. USA*, **87**, 543-547.
8. Lacourciere, G. M., and Stadtman, T. C. (1999) *Proc. Natl. Acad. Sci. USA*, **96**, 44-48.
9. Kubala, M., Plasek, J., and Amler, E. (2003) *Eur. Biophys. J.*, **32**, 363-369.
10. Krepkiy, D., and Miziorko, H. M. (2005) *Biochemistry*, **44**, 2671-2677.
11. Wolfe, M. D. (2003) *IUBMB Life*, **55**, 689-693.
12. Patteson, K. G., Trivedi, N., and Stadtman, T. C. (2005) *Proc. Natl. Acad. Sci. USA*, **102**, 12029-12034.
13. Simonds, W., Koski, G., Streaty, R. A., Hjelmeland, L. M., and Klee, W. A. (1980) *Proc. Natl. Acad. Sci. USA*, **77**, 4623-4627.
14. Hiratsuka, T., and Uchida, K. (1973) *Biochim. Biophys. Acta*, **320**, 635-647.
15. Kim, I. Y., and Stadtman, T. C. (1994) *Proc. Natl. Acad. Sci. USA*, **91**, 7326-7329.
16. Capieaux, E., Rapin, C., Thines, D., Dupon, Y., and Goffeau, A. (1993) *J. Biol. Chem.*, **268**, 21895-21900.
17. Ogasavara, Y., Lacourciere, G., Ishii, K., and Stadtman, T. C. (2005) *Proc. Natl. Acad. Sci. USA*, **102**, 1012-1016.
18. Low, S. C., Harney, J. W., and Berry, M. J. (1995) *J. Biol. Chem.*, **270**, 21659-21664.
19. Mullins, L. S., Hong, S.-B., Gibson, G. E., Walker, H., Stadtman, T. C., and Raushel, F. M. (1997) *J. Amer. Chem. Soc.*, **119**, 6684-6685.
20. Kim, I. Y., Veres, Z., and Stadtman, T. C. (1993) *J. Biol. Chem.*, **268**, 27020-27025.
21. Tamura, T., Yamamoto, S., Takahata, M., Sakaguchi, H., Tanaka, H., Stadtman, T. C., and Inagaki, K. (2004) *Proc. Natl. Acad. Sci. USA*, **101**, 16162-16167.
22. Martin, D. W., and Sachs, J. R. (2000) *J. Biol. Chem.*, **275**, 24512-24517.
23. Ko, Y. H., Tomas, P. J., and Pedersen, P. L. (1994) *J. Biol. Chem.*, **269**, 14584-14588.
24. Soti, C., Vermes, A., Haystead, T., and Csermely, P. (2003) *Eur. J. Biochem.*, **270**, 2421-2428.